University of Arizona

Department of Physics

Gamma Ray Spectroscopy - Attenuation and Compton Scattering

Maxwell Rizzo

PHYS 382 - Experimental Methods

Supervisors: Dr. John Schaibley, Will Price, Jingwei Liu

Lab Partner: Hina Goto

A report submitted in partial fulfilment of the requirements of
the University of Arizona for the degree of
Bachelor of Science in *Physics*

Submitted March 21, 2023
Data taken on Feb 13, 20, 27

Abstract

Gamma rays are high energy photons produced during the hottest and most energetic events in our universe. Supernovae, Neutron Star collisions, Black Hole accretion and Pulsars are some examples of galactic Gamma ray production. On Earth, Nuclear Fission provides a source of high energy gamma ray photons for free, as it is a spontaneous decay from a high energy to a lower energy state. These high energy photons can be extremely dangerous and should be studied with a high level of caution, but with low power radioactive sources, safe measurements and science can be conducted. This project used a $5\mu C$ Cs-137 source from 2006, and a significantly stronger source to produce gamma ray photons for compton scattering. The spectrum of $Cs-137$ is well known, and was utilized for instrument calibration. Three tests were conducted after calibration in total to study the gamma ray photons: intensity vs distance ($1/r^2$), intensity vs distance through lead (I_0e^{-ux}), and Compton Scattering with aluminum.

Contents

Chapter 1

Introduction

1.1 Background

Gamma rays include the upper end of the energy spectrum for photons. Higher energy and shorter wavelength than X-Rays, the longest wavelength gamma rays is about 10 Angstroms. Gamma rays begin at energies around 100 keV, while slightly lower energies are classified as X-Rays. Gamma rays include all photons with wavelengths shorter than 10 Angstroms, and energies higher than 100 keV. High energy gamma rays in the TeV range have been observed from special events, specifically Quasars.

Gamma rays were originally discovered in 1900 by Paul Villard discovered gamma rays while studying radium. Later, it was named gamma rays for its ability to penetrate matter more efficiently than other wavelength of photons. As it turns out, many radionuclides emit a significant amount of gamma ray radiation during nuclear decay. During many different types of radioactive fission decay, B decay, α decay, and γ decay, gamma rays are produced (1). A common production mechanism for gamma rays is through fission producing an excited daughter nucleus, which will quickly decay to a lower energy state through emission of a high energy gamma ray photon (1, 4). Nuclear fission is a naturally occurring process, and very commonly observed with many substances that are in excess on the Earth.

While historically, and in the present, the easiest production method of gamma rays is through using a long lifetime radioactive source. They provide effectively "free" production of gamma rays and other ionizing radiation, albeit decaying and losing mass. In 1963, it was discovered that Compton scattering of high energy electrons with high energy laser light could produce gamma ray photons in a controlled manner (3). In the following years, this method was refined and the first γ-ray facility was built using Compton-back scattering in order to produce a steady beam of high energy photons, as opposed to stochastic decay. Following these developments, gamma ray facilities can now produce fairly steady beams of gamma ray photons in the MeV to GeV range (3), which is extremely useful for Nuclear Physics, Medical Physics, and radiation study. Recently, in 2016, lab produced γ ray beams have been used to observe the gamma-gamma self-interaction, producing electron-positron pairs (6), using a steady stream of GeV photons.

Overall, producing higher and higher energy photon beams, or lasers, is a consistent and ongoing goal of physics. It is only useful in nuclear physics, in laser confinement, and a multitude of other uses in semiconductors. Additionally, it is very applicable to Medical Physics, as producing consistent high energy radiation, precisely targeted, is very desirable for cancer treatment. The study of high energy radiation is very important to almost every field in one way or another, there even is evidence our own body uses gamma rays in some biological processes.

The goal of this lab was to study a few different aspects of gamma ray photons, and gamma ray photon production. The source used was a $5\mu C$ Cesium-137 source, measured in December 2006. Cesium-137 is not stable, and decays with a half-life of 30.2 years (4) into

Ba-137. The gamma ray emitted then, is not technically emitted by a Cesium atom. The majority of Cesium-137 (95%) decays into Barium-137 through $\beta-$ decay, which is then in an unstable excited state. The majority of the Ba-137 (85%)then decays into a stable state through spontaneous emission of a high energy γ ray at 661.7 keV. The Barium decay has a half life of 2.55 minutes (4). So, the majority of Cs-137 decays into Ba-137 through β and γ decay, producing a γ ray with energy 661.7 keV.

Overall, the main goals of this experiment were to measure three different effects using a scintillation detector. The first experiment measured the relationship between radiation intensity and distance between the source/detector. This first experiment seeks to test the assumption that the source is emitting uniform (random) plane waves, which is the well known inverse-square law of wave propagation. The second experiment tests the relationship between radioactive intensity and distance through lead, which seeks to show that the intensity decays exponentially. The third experiment is the famous Compton scattering experiment, where the high energy gamma ray photons are scattered against electrons, changing the wavelength and energy of the incoming gamma ray.

Figure 1.1: Cs-137 Sources

Chapter 2

Experiment Setup and Theory

2.1 Lab Pictures

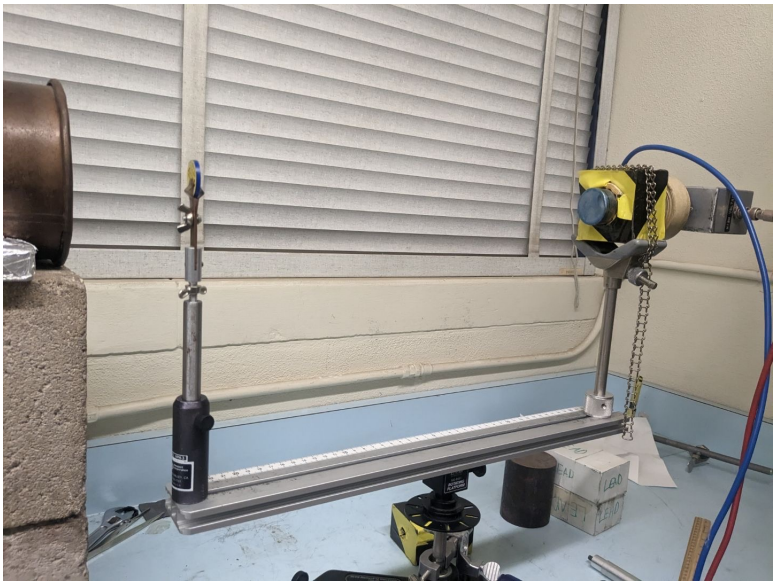

Figure 2.1: Distance Experiment

Figure 2.2: Lead Penetration Experiment

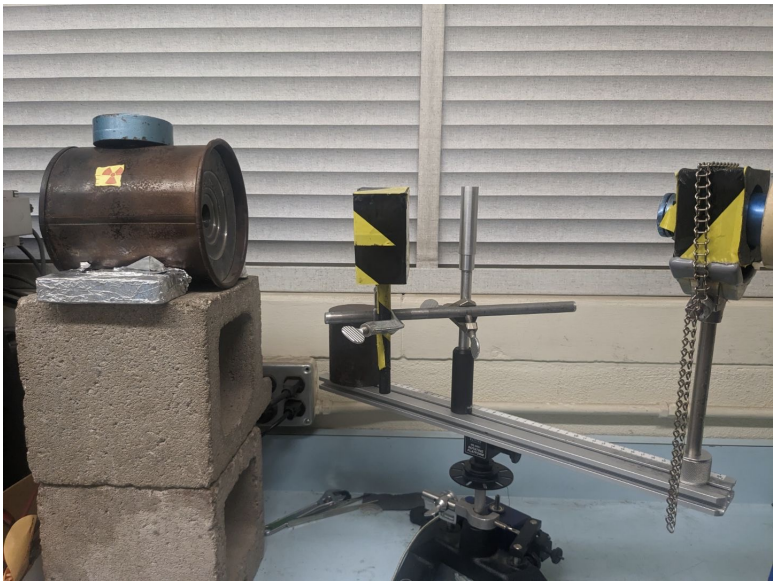

Figure 2.3: Compton Scattering Experiment

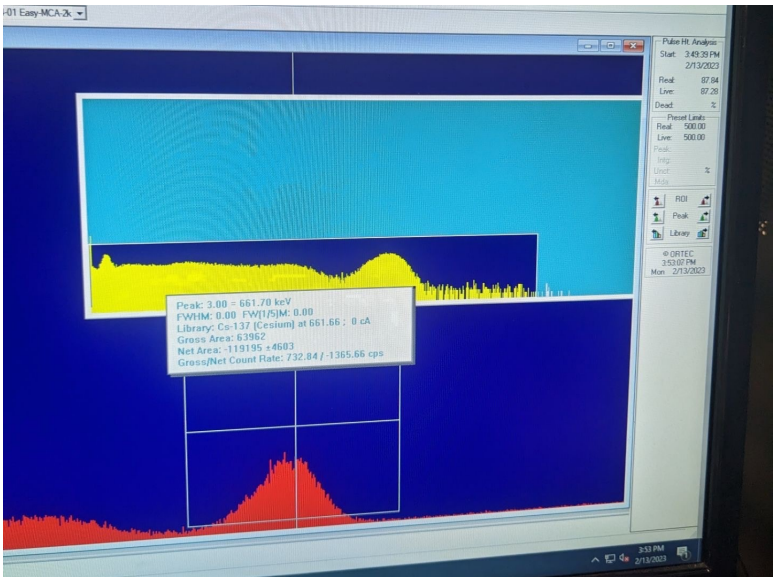

Figure 2.4: Detector Software Calibrating

Figure 2.5: PASCO Rotator Reading

2.2 Simple Apparatus

Section 2.1 has a few pictures of the in-lab setup. Figure 2.1 shows the scintillation detector and Cs-137 source together, mounted along a rail to allow for easy movement of the two objects. Figure 2.2 shows the higher power γ radiation source contained in the cylindrical lead container, with a 0.6 cm thick sheet of lead in between the source and detector. Figure 2.3 shows the setup used for the Compton Scattering experiment. The high power source was again used, in order to obtain a clearer energy spectrum. The detector was mounted along the rotating rail with the aluminum rod in between, to provide electrons to scatter the γ rays. The rotator allowed to collect data at different angles with respect to the scattering rod.

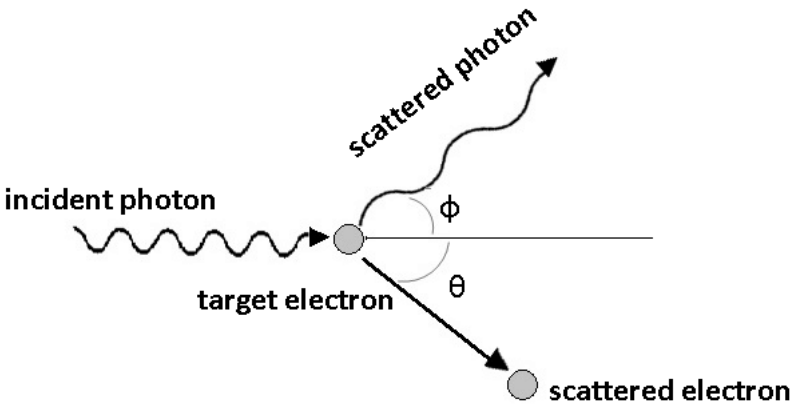

Figure 2.6: Compton Scattering Interaction

The target electrons are provided by the aluminum rod, which is at rest in between the source and detector. The detector maintains mounted on the rotator, and can move to different angles with respect towards the central axis, measuring scattering at different angles with respect to the incident γ ray photons.

2.3 Detector Efficiency

The scintillation detector used was NaI (Sodium Iodide). Recent developments have improved the availability of cheap NaI detectors, allowing for gamma ray spectroscopy to be done. While the detector is fairly functional it requires software to operate, in order to do background subtraction and calibration to obtain energy spectra (Counts per second versus photon energy). Additionally, it is not going to be anywhere close to $\%100$ efficiency, a significant portion of the γ photons will penetrate through the detector, with no interaction/detection. The detector works using a photocathode, a certain percentage of the γ ray photons will forward Compton scatter using the process pictured above. The forward scattered electron is propagated down a photo-multiplier tube, where a careful proportion is worked out for the final electron cloud being non-linearly proportional to the incident energy of the γ ray photons. Considering all this, it is possible to work out the theoretical efficiency of the detector, using our lab-measured low-power radiation source.

This process requires photo multiplying, and redistributing large amounts of charge/voltage across the detector plane. So, there is a time constant associated with this process, and the detector has a chance to have "dead time" where it is not actively collecting data. "live

time" is the exact opposite, the time where the detector is on, functional, and reading data from its interactions. "real time" is effectively the sum of the two. The software does this automatically, but it goes to keep in mind that when calculating "decays per second" or cps, the proper equation is to divide the total counts by the total "live time", because there were no counts recorded during the dead time. For detector efficiency calculation, however, using the real time to calculate count rate makes more sense, as that factors in the live/dead time into the efficiency of the detector. For everything else, it makes more sense to use "live time". In practice, this point is not critically important as the detector operated very well, around 99% live time during our 10 minute data collection trials, so there was almost no need for this consideration. The difference between real and live times were negligible.

The Cs-137 (τ_{half} = 30.2 years) source used had an activity of $5\mu C$ when measured in December 2006. This can be converted to "counts per second"(cps) or equivalently "decays per second". The conversion factor is $1\mu C = 37000$ cps. So, in theory the $5\mu C$ source equates to $A_0 = 185,000$ cps. This is the initial activity measured in 2006, to get the current day theoretical activity, it must be evolved in time using the exponential decay law, as the mass loss is proportional to how much mass there is.

$$A(t) = A_0 e^{-\lambda t}, \lambda = \frac{ln(2)}{\tau_{half}}$$

Plugging in the values for Cs-137, τ_{half} = 30.2 years, and approximately 17 years passing since A_0 was measured in 2006, it gives $A(t_{present}) = 125,233$ cps, which represents the current, present day activity of the $5\mu C$. Placing the source directly upon the detector takes up half of all solid angles the source can radiate through, so it can be assumed that half of the γ radiation is going away from the detector, and half into it. Dividing the present theoretical activity of the source by 2 gives $62,616$ cps entering the detector. After waiting for a maximum length data collection trial (500 seconds) the experimental count rate recorded by the NaI detector was $A_{exp} = 13,142$ cps. Dividing these two values yields the detector efficiency, e,

$$e = \frac{A(t_{pres})_{exp}}{A(t_{pres})_{theor}} = \frac{13,142}{62,616} \approx 21\% \text{ efficient.}$$

This is a reasonable value for the NaI scintillator, and contextualizes the difficulty at measuring γ ray photons, they do penetrate most materials after all. This value was not used for the following analysis in the rest of the lab, as the efficiency is assumed to be constant between experiments/collection trials.

2.4 Cs-137 Spectrum

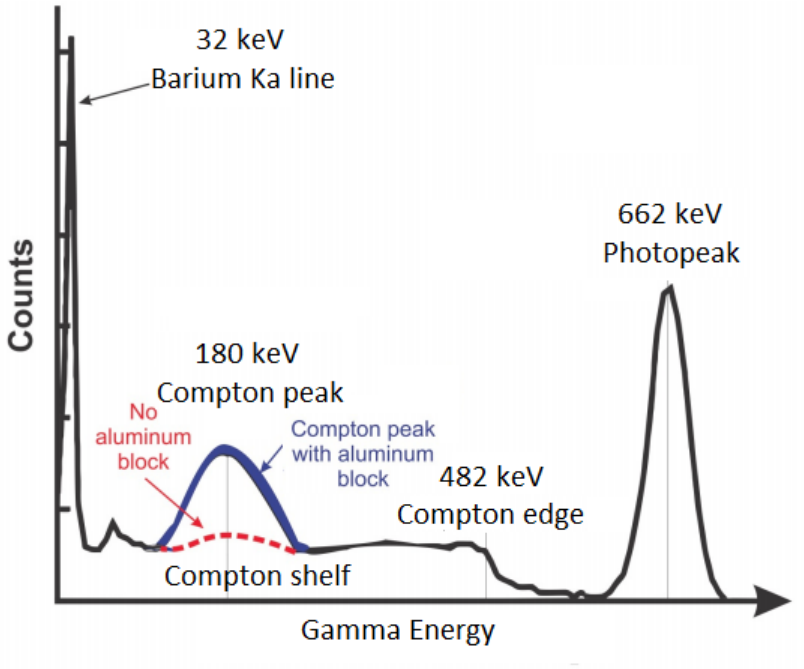

Figure 2.7: Cs-137 Spectrum (4)

Figure 2.7 shows the expected Intensity (cps) spectrum from Cs-137 (4). There is a large low energy peak, corresponding to a low energy photon emitted by the β decay process. There is a large photopeak corresponding to the dominant γ decay process at 661.7 keV. This peak is what is used for energy calibration of the NaI instrument. In between the two main emission lines, there is a continuum caused by Compton scattering. Compton scattering within the NaI detector produces this "Compton shelf" even when the aluminum block is not present. The Compton peak added to the Compton edge will always give the energy of the main γ ray photon, which makes sense by conservation of energy. This is the expected spectrum to be observed for the Cs-137 source on the NaI detector, and was closely matched in the experiment.

2.5 Experiment 1 - Distance

The first experiment was testing the geometric property of the inverse square law. The inverse square law applies to a large source of phenomena, really because it is a geometric property. Any source that produces a local field strength on a surface, must have the local field strength drop off according to $1/r^2$, as the surface area of the sphere is increasing according to r^2. As long as the field source is emitting in a uniform distribution, this property holds, as the only assumption is spherical symmetry, propagation, and conservation of energy. While the radioactive source used is stochastic, random, every γ ray emitted along a random solid angle, this produces a fairly homogeneous distribution of emission versus solid angle, as it emits along all angles equally. So, this assumption is valid, the γ rays propagate outward, and if energy is conserved locally (usually it is), the intensity of the beam must drop off according to $1/r^2$.

Intensity and cps are analogous and proportional to one another, by the energy of the photon beam, for Cs-137, the γ photopeak occurs at 661.7 keV.

The working equation to be fit towards the data to show that it exhibits this behavior is built with three parameters. A_1 is the present day activity (cps) of the source with some factors of distance built in, d is the position of the NaI photocathode array, and A_{bkg} is the background level that was present in our data, which will be discussed later. The inverse square law model with an offset, and a background level becomes,

$$A_{exp}(x) = \frac{A_1}{(x-d)^2} + A_{bkg},$$

where x is the position along the rotator. If the source was placed against the detector, such that $x = d + L$, where L is the length of the detector, about 7 cm, the distance from the cap to the photocathode plane, then $A_{exp}(d+L) = A_1/(L)^2 + A_{bkg} = A_{0exp} = 13,142$ cps from above. This gives a theoretical basis for the fit parameters. Additionally, the detector was behind the 20 cm mark, so the fit parameter d should be larger than 20 cm. All three parameters can be compared to their best fit experimental value.

2.6 Experiment 2 - Lead Attenuation

The second experiment was testing the penetration property of the high energy γ rays through lead sheets, a common shielding material for high energy radiation. A higher power source was used in place of the $5\mu C$ Cs-137 source, it was also Cs-137, but significantly higher power, around $125\mu C$. The higher power source was used in order to have a larger range of attenuation, to observe a large dynamic range of attenuation. Lead sheets were progressively placed in front of the high power radioactive source. In theory, the placement of the plates along the path should not affect the attenuation, however due to Compton scattering and back scattering, the placement does matter in practice. It was decided that placing the lead sheets closest to the source, and furthest from the detector, would reduce the likelihood of Compton scattered photons to make it into the detector. Both placements were tested for a single sheet, and no difference was observed. The attenuation of γ ray radiation (shielding) can be described by the following equation (5),

$$I(x) = I_0 e^{-\mu x} + I_{bkg}.$$

Here 3 parameters are required for the fit again. I_0 is the intensity (or cps) measured by the detector with no lead sheets in the path, μ is the absorption coefficient, and is represented by $\mu = \alpha\rho$, where $alpha$ is the mass absorption coefficient (cm^2/g), and ρ is the density of the absorber (g/cm^3). I_{bkg} is the background activity level for the source x is the total lead sheet thickness. The intensity or activity of the higher power source is not know accurately, so that parameter is not constrained, but the absorption coefficient can be compared to accpeted values.

2.7 Experiment 3 - Compton Scattering

Figure 2.6 shows a simple diagram of the Compton Scattering interaction. The incident photon scatters off a target electron, in this case the electrons can be considered to be at

rest. Both the photon and electron are scattered at random angles and energies, producing a continuous spectra of intensity vs energy, instead of a clearly defined photopeak. To derive the shift in photon energy as a function of photon scattering angle, conservation and momentum and energy will be appealed to in this situation. Conserving momentum gives,

$$\vec{p_0} = \vec{p_1} + \vec{p_e},$$

Where $\vec{p_0}$ is the initial momentum of the photon, $\vec{p_1}$ is the scattered photon momentum, and $\vec{p_e}$ is the scattered electron final momentum. Rearranging the equation and squaring both sides gives

$$p_e^2 = p_0^2 + p_1^2 - 2\vec{p_0}\vec{p_1} = p_0^2 + p_1^2 - 2p_0p_1cos(\theta).$$

Where θ is the scattered angle of the photon. Conserving energy gives the expression, $E_{phot} = pc$

$$p_0c + m_ec^2 = p_1c + (m_ec^2 + p_e^2c^2)^{1/2}.$$

Moving p_1c to the other side, and squaring both sides of the equation gives,

$$(p_0 - p_1)^2c^2 + m_e^2c^4 + 2mc^3(p_0 - p_1) = (m_ec^2 + p_e^2c^2),$$
$$p_e^2 = p_0^2 + p_1^2 - 2p_0p_1 + 2m_ec(p_0 - p_1).$$

Using both these expressions to eliminate p_e^2 gives,

$$m_ec(p_0 - p_1) = p_0p_1(1 - cos(\theta)).$$

Multiplying both sides by $h/p_0p_1m_ec$ cancels the prefactors on the left side and leaves the expression with just the difference in $h/p = \lambda$, so,

$$\lambda_1 - \lambda_0 = \frac{h}{m_ec}(1 - cos(\theta)).$$

Using $E = hc/\lambda$ and rearranging, the equation can be solved for the energy shift,

$$E_1 = \frac{E_0}{1 + \frac{E_0}{m_ec^2}(1 - cos(\theta))}.$$

This derivation followed that from Tipler (2, 3), and are Compton's Equations. These equations are equivalent, but for ease of use and fitting purposes the shift in wavelength will be used. There is only one the change in wavelength can be fit against $1 - cos(\theta)$, and the slope should in theory be $\frac{h}{m_ec}$. There is only one free parameter in this fit, and is again constrained theoretically and will be compared to the experimental result.

2.8 Procedure

The pictures above in section 2.1 give a good idea of the procedure. First, the NaI detector had to be configured with the proper amplifiers, power supplies, and interface to a nearby computer with the detector software running on it. After ensuring that the detector is both on, functional, and reading out meaningful data, data collection runs can begin. Initially, we

thought that it was a requirement to calibrate the detector with respect to the photon energy before the data collection runs. We learned that was not completely necessary, it is possible to calibrate after the data collection, as long as the main photopeak was defined and present. For the first experiment, following Figure 2.1, the low-power Cs-137 source was mounted on a rod along the rotator, parallel with the NaI detector. This allowed for the Cs-137 source to slide back and forth along the rotator, changing the distance from the detector while maintaining alignment along the detector axis. The activity (cps) would stabilize after around 100 seconds, so each trial was around that long before recording the activity at that certain distance. Overall, 11 different data points were collected, at 11 different distances from source to detector. More data points were collected, but we made a mistake by accidentally including the low energy and Compton shelf photons in our activity measurement for the first attempt. We had to throw out a significant amount of data because we did not save the first attempts, in hindsight it is extremely valuable to save every single data run. While tedious, the detector software's best functionality is the ability to recall previous data sets, and do active analysis like it was collected once again. Overall, we recorded the activity of the source (cps) at 11 different distances, only considering the photons within the γ photopeak.

For the second experiment, looking at Figure 2.2, the higher power Cs-137 source is present inside the dark lead cylinder housing on the left. There is a single lead sheet present in front of the source housing, around 80 cm to the right lies the NaI detector. The activity was recorded for 0 lead sheets, up to 6 lead sheets, or around 4 cm of lead. Each trial was recorded for the maximum time allotted by the detector (500 seconds). This experiment was fairly straight forward, record the activity, add a sheet, repeat.

For the third experiment, looking at Figure 2.3, this was the famous Compton Scattering experiment. The high power source was again used in the large cylindrical lead housing. It was mounted in line with the rotator and NaI detector. As there is a lot of scattering and direct detection happening, in order to have a spectrum of the pure compton peak, a background subtraction method was used. For each angle, first a dataset was collected where the aluminum rod was absent. Next, the aluminum rod was placed along the main rotator axis to scatter the γ rays. The software has the ability to preform a background subtraction, taking the scattering dataset and subtracting off the dataset without the rod present. This leaves the spectrum of solely the Compton peak corresponding to the scattering done by the aluminum block, in theory. Figure 2.7 shows the Cs-137 spectrum, with the blue curve representing the change in spectrum from the presence of the aluminum rod. Subtracting the dataset without the rod from the one with the rod leaves solely the compton peak. This allows for the software to peak find the Compton peak to high accuracy, obtaining the change in Energy or wavelength, for the Compton peak at that specific angle. This was done at 0 degrees, and 5 other non-zero angles, which provides data points to be plotted for the change in wavelength against the function of angle. Both the scattering dataset and background dataset were collected using the maximum exposure time (500s), meaning a single angle took around 20 minutes. This meant that only 9 angles could be done in the entire lab session, assuming 100% efficiency in data collection. Only 6 were collected, as we did make a mistake on one angle and had to repeat it, costing us significant amount of time. The results are expected to be tenuous at best, as it is difficult to obtain the scattering spectrum with only 6 data points. The general procedure was to do an exposure at an angle, then repeat the same angle with the aluminum block in, save both data sets, and then move to the next angle. The calibration, and subtraction or "trimming" can be done afterwards as long as the datasets are saved.

Additionally, seen in Figure 2.3 on the left of the Aluminum rod is a large lead block.

Due to the wave propagation of the photons and Huygens's principle, the photons exiting the detector do not stay in a concentrated beam. Instead, they diffract and propagate outwards in spherical wave fronts. This is an issue for the compton scattering experiment, as goal is to only detect the scattered photons at an angle, and not the γ ray directly from the source. The lead block is a make-shift solution, but may have been the main contributor to this experiment not producing accurate data. The lead block was positioned carefully for each Compton scattering data collection, in order to block the photons from pathing directly from the source to the detector. This reduces the direct photons detected, and increases the percentage of detected photons that were Compton scattered by the rod. It was a make-shift solution, in that it was almost impossible to have the block completely block the direct path to the detector, while not obscuring the path to the rod. This was a problem, and I believe the reason for the bad data. Small angles were very difficult to use the lead block, while larger angles were easier, which potentially offset the entire Compton effect itself. If this experiment were to be redone, more careful consideration would go into the lead blocker. Requiring manually resetting the position of the heavy apparatus and blocks, it is likely the data is heavily contaminated by this effect.

The NaI detector came with a software called MAESTRO, which was fairly functional. As aforementioned, the ability to save datasets and calibrate/analyze after the fact is very useful. The procedure in general with MAESTRO was fairly straight forward, ensure the device was identified and connected, and begin data collection. MAESTRO allows for calibration of energy spectrum, using the known energy of the large photopeak. It automatically calculated the activity (cps) for each data collection using the "live time" of the detector, along with the associated error for the peak. Using the calibration, region marking and peak finding, the software can integrate the amount of counts under the peak to a reasonable width. For the first 2 experiments the γ photopeak was of interest, which was fairly straight forward to calibrate and identify. The third experiment required trimming and background subtraction, detailed above.

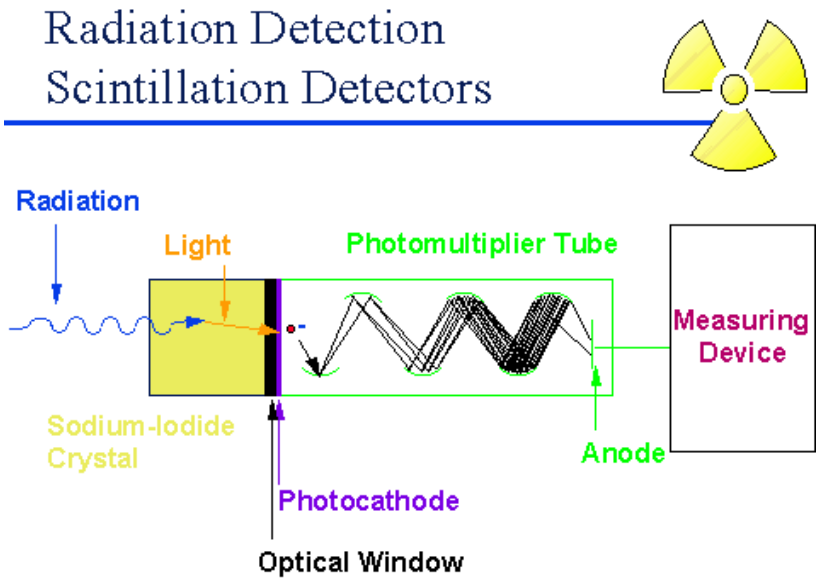

Figure 2.8: Schematic of standard NaI Scintillation Detector credit: *Nevada Technical Associates*

Chapter 3

Results

3.1 Experiment 1 - Distance Results

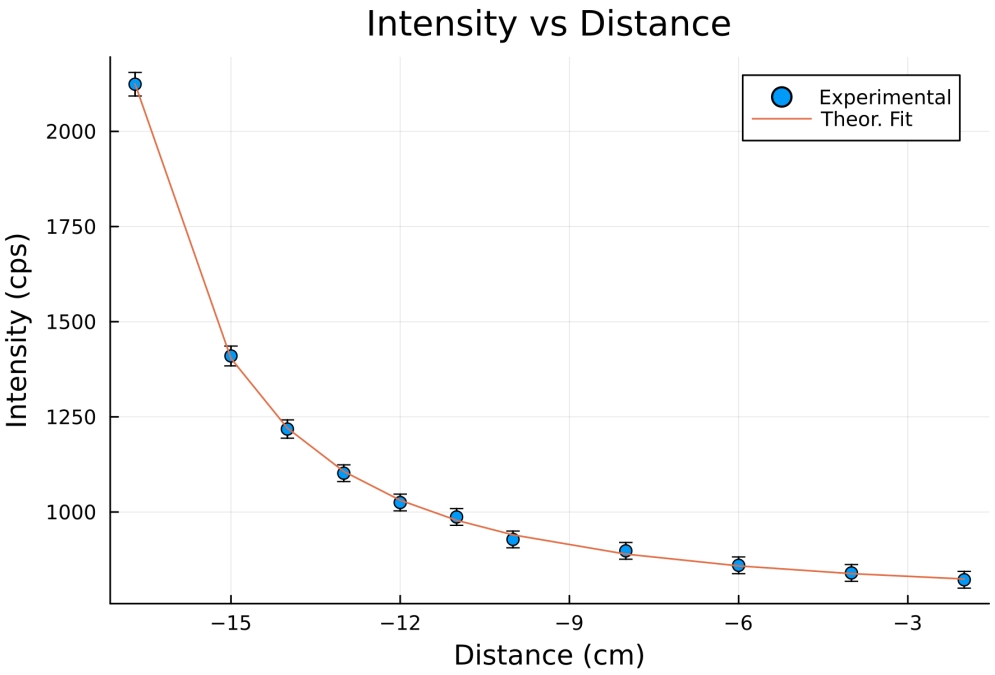

Figure 3.1: Cs-137 Intensity vs distance

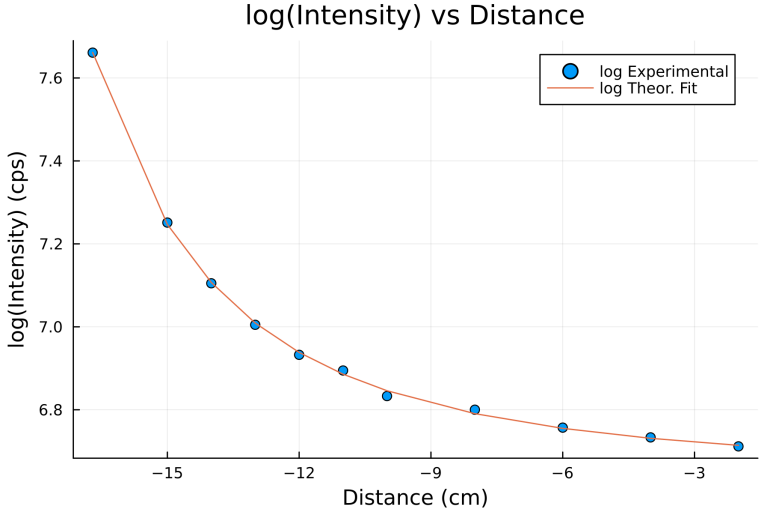

Figure 3.2: Cs-137 log(Intensity) vs distance

Figure 3.1 is the intensity of the of the source with respect to distance, while Figure 3.2 is the log of the intensity vs distance. This shows that it is a power law, and not an exponential, as the log plot is nonlinear. The reason the distances are negative is because decreasing x meant moving further away from the detector. Figure 3.1 shows a fairly good result, the intensity vs distance curve closely matches the model,

$$A_{exp}(x) = \frac{A_1}{(x-d)^2} + A_{bkg}.$$

The χ^2 least-squares fit found the parameters to be

$$A_1 = 18332.29 \pm 26.87\ cps * cm^2, d = -20.38 \pm 0.0026\ cm, A_{bkg} = 769.79 \pm 0.2078\ cps.$$

The fit value for d, the distance from the origin to the photocathode plane, looks accurate. It was speculated to be at least greater than 20cm away from 0 as that was where the detector was mounted. The negative sign is just because the x axis was setup backwards. Now to check, from above $A_{exp}(d+L) = A_1/(L)^2 + A_{bkg} = A_{0exp} = 13,142$, so,

$$L = \frac{A_1}{(A_{0exp} - A_{bkg})})^{1/2}.$$

Plugging in A_{bkg} from the fit, A_{0exp} and A_1 from the calibration, and gives $L = 1.217$ cm, which is the distance from the cap of the NaI detector to the photocathode plane. I estimated this earlier to be 7cm, which was significantly far off. This value for L makes sense, and further verifies the fit value for d. The fit parameter d is very close to 20 cm, which was almost exactly where the front of the detector was mounted. The distance from the origin to the photocathode plane, d, being about centimeter larger than where the detector was mounted verifies the determined value of L. If L was measured beforehand, and accurately, it would allow for the theoretical determining of A_1 and d, instead of the other way around.

Overall, the fit matches the data very well. The fit passes through each data points error bar, which is a good rule of thumb. The intensity vs distance very closely matches that of the inverse square law, with an offset in position and a background level. We are not sure why the background level is present at all in the data. MAESTRO should automatically preform background subtraction on any constant signal, making it so the baseline is 0, instead of 770 cps. This could have been caused by the presence of the other radioactive sources in the lab not fully being shielded, which is the only plausible explanation. This experiment closely verifies the geometric inverse square law for spherically propagating homogenous radiation.

3.2 Experiment 2 - Lead Attenuation

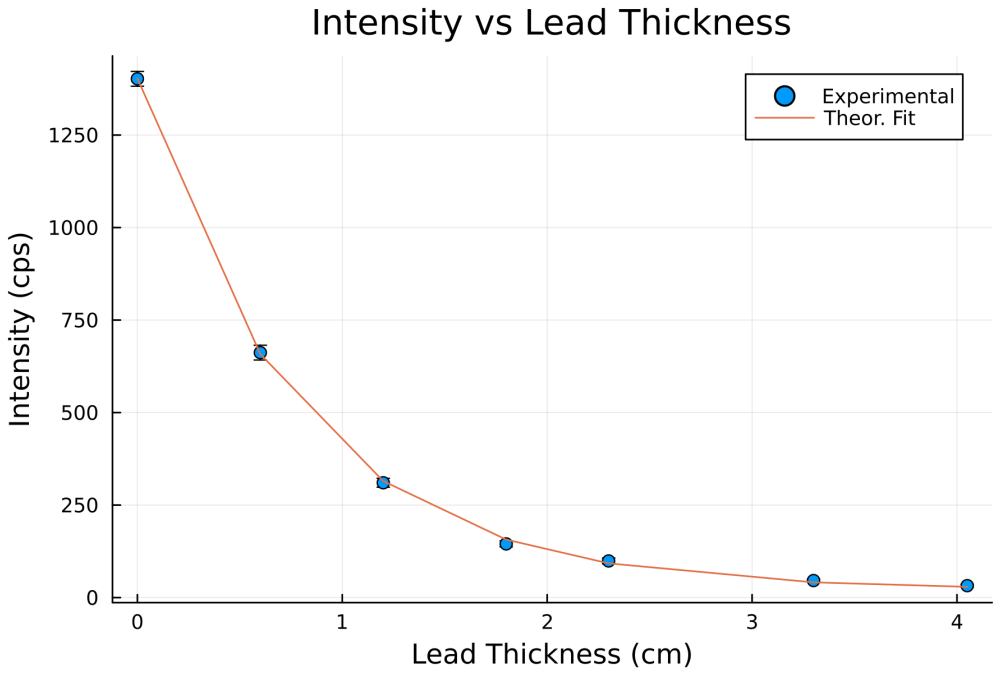

Figure 3.3: Cs-137 Intensity vs Distance through Lead

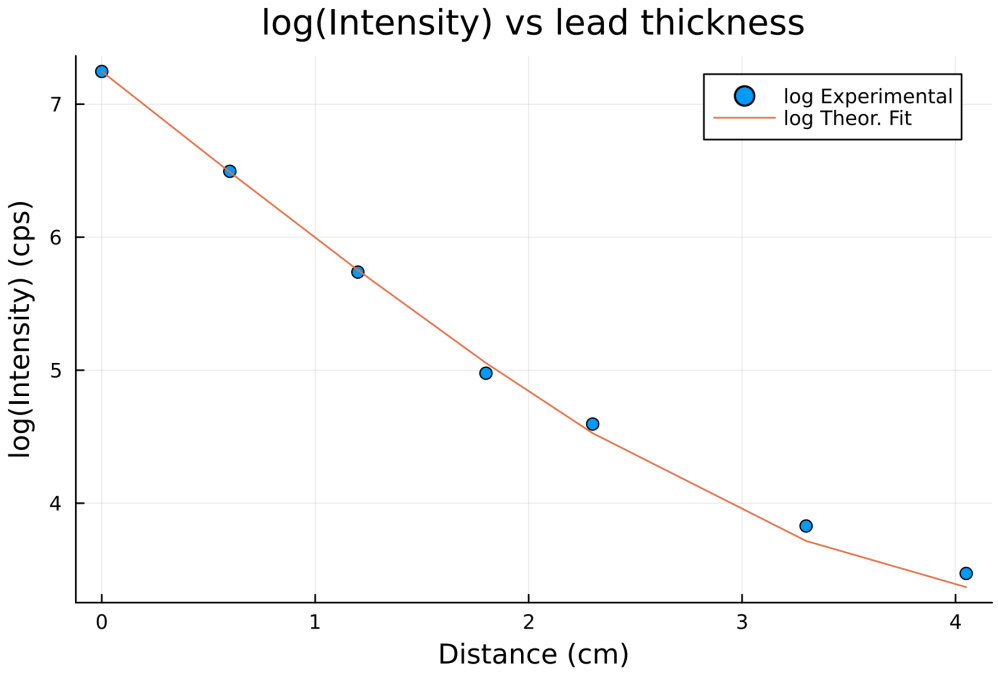

Figure 3.4: Cs-137 log Intensity vs Distance through Lead

Here are the results of the intensity of the Cs-137 γ ray photon plotted against distance propagated through lead. The second plot is the log of the intensity vs distance, which is linear, meaning that the first relationship must have been an exponential decay. The first plot is very similar to experiment 1, but the logarithm plot clearly shows the difference in behavior.

The results here look very promising, the logarithm plot is very closely linear, supporting the exponential decay model,

$$I(x) = I_0 e^{-\mu x} + I_{bkg}.$$

The χ^2 least-squares fit found the parameters to be

$$I_0 = 1381.34 \pm 0.488\ cps, \mu = 1.292 \pm 0.0011\ cm^{-1}, I_{bkg} = 21.668 \pm 0.411\ cps.$$

Clearly this must be a much higher power source, as we observed around $1,400$ cps from the source across 80 cm. The lower power source was observed around $14,000$ cps across 1.217 cm. The ratio of distances is around 80, so it would be expected to observe $14,000/(80^2) = 2$ cps across 80 cm, instead of the $1,400$ cps actually observed. So, the high power source must be at least 700 times more powerful than the lower power $5\mu C$ Cs-137 source. I_{bkg} is very close to zero, which is a much better result than the first experiment which had a significant background.

The best fit absorption coefficient, $\mu_{exp} = 1.292$ cm^{-1} $= \alpha\rho$, where for lead at $E = 0.66$ MeV, and the mass absorption coefficient $\alpha = 1.248e^{-01}$ cm^2/g, and the density $\rho = 11.33$g/cm^3, gives $\mu_{theor} = 1.414$ cm^{-1}. Both the absorption and mass absorption coefficient depend on the energy of the incident photon, a lookup table was used from NIST, corresponding to the photopeak of the Cs-137 γ ray. The best fit absorption coefficient is very close to the theoretical absorption value, which is a great result for this experiment.

3.3 Experiment 3 - Compton Scattering

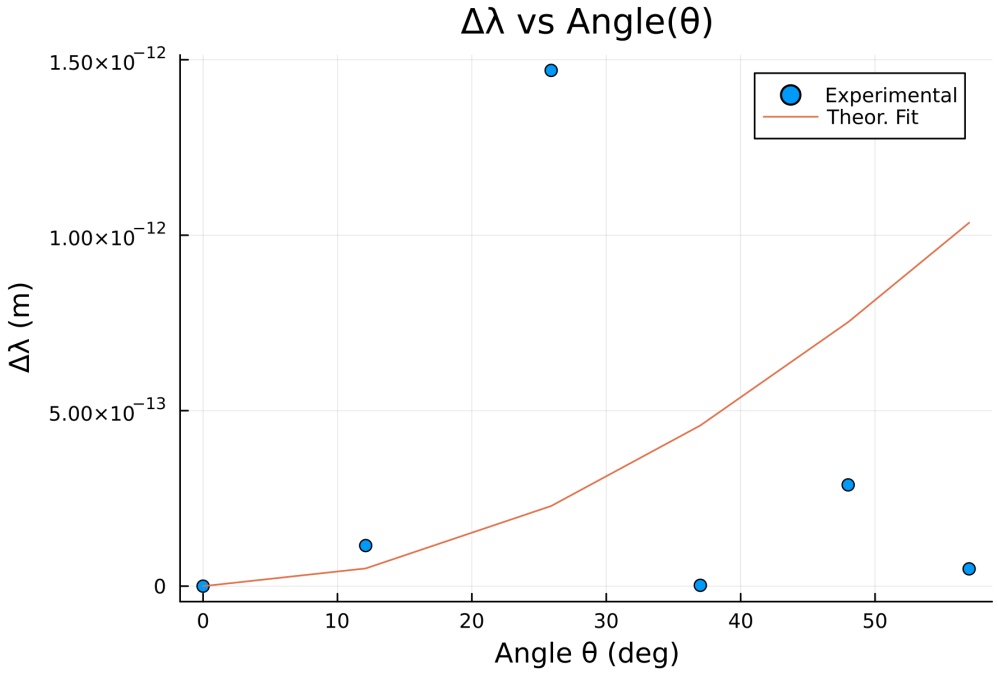

Figure 3.5: Compton Scattering Change in Wavelength vs Angle

Here are the results for the Compton scattering experiment, with the change in peak photon wavelength plotted against the scattering angle. Clearly something did not go well, and the

data is not consistent with the model. The model is represented by Compton's equations, which for the shift in photon wavelength is,

$$\lambda_1 - \lambda_0 = \frac{h}{m_e c}(1 - cos(\theta)).$$

I won't report the χ^2 best fit parameters, as clearly the fit did not converge in any meaningful sense. The plot and model does provide some useful information though. As the fit was not converging, I input the accepted values of $\frac{h}{m_e c}$, which is what the orange line is plotting. The orange line on figure 3.5 is not a fit at all, but Compton's equation with the correct natural constants inputted. So it essentially is a perfectly theoretical dataset, showing what the data should look like if it was taken correctly, or the procedure refined significantly. The first two data points look reasonable, but after that there is a massive difference between the theory and the experiment. Coincidentally, from the third data point and on was exactly when we started using the lead block. This further confirms my suspicion that the lead block was not functioning in a controlled manner between experiments, and left a lot of leeway to the configuration/geometry. The model shows that the scattered wavelength is always greater, so the photon is lower energy, and the greater the angle the greater the loss in momentum. This is the expected result, and confirms our conservation equations earlier.

This part of the experiment was very difficult, not only from the apparatus, but also from every single data point requiring 20 minutes of data collection. It makes it very difficult to collect a large amount of points in any timely manner. This perhaps may motivate the creation of a more automated apparatus, or a fully automated one, that can preform and scan in angle by itself, not requiring a lab technician to constantly reset apparatus. The apparatus definitely needs improvements to the lead block technique in order to obtain a meaningful result.

3.4 Summary

Overall, the results of these experiments involving high energy γ ray photons was fairly successful. The first two experiments, the effect of distance ($1/r^2$) and exponential decay/attenuation through lead shielding matched their models closely and produced convincing results. The Compton scattering experiment was by far the most difficult, due to the manual nature of tedium, and requiring precise reproducible setups to have meaningful data. The Compton scattering experiment was largely unsuccessful, our data does not match the model to any meaningful degree. While the third experiment was the most difficult and yielded rough results, it still allowed for a significant amount of theory and analysis on what failed.

Chapter 4

Discussion and Analysis

4.1 Limitations

While this experiment was fairly successful, it was a bit limited in scope. Experiment 1 and 2 were both very successful, but both only contained around 10 data points each, which is not exactly enough to make great comparisons to accepted values. Also, it can create artifacts, misrepresent the true nature, and miss fine structure that occurs from sampling many data points. Experiment 1 could have had double the data points, but we made an early mistake and had to toss out the first half. Time was constantly against us, limiting how many data points were obtainable in a single lab session. Similarly for Experiment 2, it would have been fairly straight forward to obtain more data points, and higher resolution plots, but time was of the essence.

Lastly, Experiment 3 (Compton Scattering) was very difficult procedurally. As aforementioned in the data analysis, the first two data points look fairly reasonable, as the lead blocker had not been put in place yet. From the third point and on, the lead blocker was in place along the apparatus, attempting to block the direct path but leave the scattering path clear. The third data point is a significant outlier, which makes sense as using the lead block for low angles is extremely difficult. For low angles the angular difference between the rod and detector is very small, leaving almost no room for the giant square lead block. For higher angles, it is potentially possible to have the block in a position that does not obstruct the scattering path, but blocks the direct path. I re-positioned the block many times and quickly realized there was no way to keep any form of consistency between the different angles/ data points. The block method clearly was problematic for this experiment, and would need to be refined before repeating.

4.2 Summary

Overall, we are very happy with these combination of experiments. We successfully demonstrated the inverse square law for propagating spherical waves, as well as demonstrated the exponential decay law through dense lead shielding. We attempted Compton scattering and obtained reasonable results that did not converge to the model, due to an experimental difficulty with the apparatus. This experiment used a NaI scintillation detector, combined with MAESTRO software to preform spectral analysis on Cs-137. We observed the full spectrum of Cs-137, the low energy peak, the Compton shelf and edge, and the main γ photopeak.

4.3 Future Work

If one were to repeat this experiment, the methodology of all of the experiments could be refined significantly. It seems possible to automate all three experiments in one way, that

a lab technician can start the collection and the device will begin, collect, the move to the next distance/angle/lead sheet and collect again. Experiment 1 would just require shifting the source linearly, 2 would require some heavy lifting of lead, 3 would be fairly easy with just rotation and shielding. I believe automation would increase the precision and accuracy of this experiment by multiple orders of magnitude. Allowing for hundreds to thousands of data points to be collected continuously in a day would make for very accurate analysis, without manual lab tech labor.

Besides fully automating all three experiments to obtain huge amounts of data, the Compton scattering experiment could be refined slightly using a better shaped shield. A small shield could be used at low angles, and a larger one at larger angles. Additionally, some form of ensuring the lead block is in a repeatable/standard position is necessary for ensuring the data points are somewhat consistent with one another.

References

[1] ARPANSA (n.d.), 'Gamma radiation', *Australian Radiation Protection and Nuclear Safety Agency* .
URL: *https://www.arpansa.gov.au/understanding-radiation/what-is-radiation/ionising-radiation/gamma-radiation*

[2] Arutyunian, F. and Tumanian, V. (1963), 'The compton effect on relativistic electrons and the possibility of obtaining high energy beams', *Physics Letters* **4**(3), 176–178.
URL: *https://www.sciencedirect.com/science/article/pii/0031916363903512*

[3] D'Angelo, A. (1998), 'Review of compton scattering projects'.

[4] Maxfomitchev (2022), 'The rich physics of cs-137 gamma spectrum', *Maximus Energy* .
URL: *https://maximus.energy/index.php/2020/10/24/the-rich-physics-of-cs-137-gamma-spectrum/*

[5] McAlister, D. (2018), *Gamma Ray Attenuation Properties of Common Shielding Materials* .

[6] Ribeyre, X., d'Humières, E., Jansen, O., Jequier, S., Tikhonchuk, V. T. and Lobet, M. (2016), 'Pair creation in collision of γ-ray beams produced with high-intensity lasers', *Phys. Rev. E* **93**, 013201.
URL: *https://link.aps.org/doi/10.1103/PhysRevE.93.013201*